

ARTICLE OPEN



Distinct and shared intrinsic resting-state functional networks in children with idiopathic autism spectrum disorder and fragile X syndrome

Dongyun Li^{1,9}, Danyong Feng^{2,3,9}, Chun Chun Hu¹, Yuxin Tian¹, Allan L. Reiss^{4,5}, Randi J. Hagerman^{6,7}, Xiu Xu¹, Zhongwei Qiao⁸, Rihui Li^{2,3} and Qiong Xu¹

© The Author(s) 2025

Autism spectrum disorder (ASD) and fragile X syndrome (FXS) are behaviorally overlapped. However, little is known about the functional patterns underlying the cognitive and behavioral characteristics of FXS and ASD. The present study aimed to identify the distinct or/and shared functional networks in young children with FXS and idiopathic ASD. We recruited 150 children consecutively in a group with FXS, a group with idiopathic ASD, and a group with typically developing (TD) children. Resting-state functional magnetic resonance imaging (fMRI) and behavioral data were collected and genetic information was obtained in the FXS group. We compared functional connectivity (FC) among the three groups and found that both FXS and ASD showed significantly decreased FC among the default mode network (DMN), sensorimotor network (SMN), cerebellum network (CN), and visual network (VN) relative to TD. FXS specifically demonstrated decreased FC within DMN, while both FXS and ASD exhibited significantly decreased FC within the CN and also between the CN and DMN, SMN, VN, respectively. Aberrant topological alterations of CN were identified in children with FXS and ASD, while ASD group showed significantly lower segregation in regions that integrate sensory and visual information, and motor coordination function. Moreover, correlations between the severity of social affect and mean FC of various cerebral-cerebellum networks in FXS exhibited significantly distinct trends from those observed in ASD. In the FXS group, the topological measure at crus I of the cerebellum is found to be negatively associated with DNA methylation levels. These results were statistically robust and demonstrated the shared and distinct profiles of intrinsic functional networks in FXS and ASD, two phenotypically overlapping developmental disorders.

Molecular Psychiatry; <https://doi.org/10.1038/s41380-025-03112-y>

INTRODUCTION

Autism spectrum disorder (ASD) exhibits a considerable degree of etiological and phenotypic heterogeneity, manifesting in a spectrum of impairments encompassing social interaction, communication difficulties, and repetitive stereotyped behaviors [1, 2]. This inherent heterogeneity poses a significant challenge in unraveling the complex mechanisms underlying ASD. Notably, approximately 20–40% of children diagnosed with ASD exhibit identifiable genetic syndromes, characterized by either ASD-associated risk genes or copy number variations (CNVs) [3]. To confront this complexity, one promising strategy involves delving into the neuropathological intricacies within a more homogenous subgroup of ASD with a confirmed genetic etiology, such as Fragile X syndrome (FXS), the leading monogenic cause of ASD [4, 5]. By studying FXS, caused by CGG trinucleotide repeats in the fragile X messenger ribonucleoprotein 1 gene (*FMR1*), we can gain insights into specific mechanisms contributing to cognitive and

behavioral symptoms, offering a focused perspective to understand broader ASD heterogeneity.

Advanced magnetic resonance imaging (MRI) provides translational opportunities to elucidate in vivo neuropathological mechanisms in humans. Previous structural MRI studies conducted on individuals with ASD have revealed abnormalities in various brain regions and tracts across the entire brain. Subcortical structures, for example, enlarged amygdala, have been observed in ASD through structural MRI [6, 7]. In FXS, consistent structural abnormalities, such as an enlarged caudate nucleus [7] and enlarged frontal gyri [8], have been reported. These reproducible structural abnormalities in FXS may implicate its distinct neuroanatomical dysfunctions relative to ASD, although both disorders share overlapping behavioral phenotypes.

Functional MRI studies (fMRI) in ASD have also reported widespread altered functional connectivity at the whole-brain level, or in intrinsic networks such as the default-mode network

¹Department of Child Health Care, Children's Hospital of Fudan University, Shanghai, China. ²Centre for Cognitive and Brain Sciences, Institute of Collaborative Innovation, University of Macau, Taipa, Macau S.A.R., China. ³Department of Electrical and Computer Engineering, Faculty of Science and Technology, University of Macau, Taipa, Macau S.A.R., China. ⁴Center for Interdisciplinary Brain Sciences Research, Department of Psychiatry and Behavioral Sciences, Stanford University, Stanford, CA, USA. ⁵Departments of Radiology and Pediatrics, Stanford University, Stanford, CA, USA. ⁶Medical Investigation of Neurodevelopmental Disorders (MIND) Institute, University of California Davis, Sacramento, CA, USA. ⁷Department of Pediatrics, University of California Davis School of Medicine, Sacramento, CA, USA. ⁸Department of Radiology, Children's Hospital of Fudan University, Shanghai, China. ⁹These authors contributed equally: Dongyun Li, Danyong Feng. ✉email: zqiao@fudan.edu.cn; rihui@um.edu.mo; xuqiong@fudan.edu.cn

Received: 8 October 2024 Revised: 14 May 2025 Accepted: 7 July 2025

Published online: 15 July 2025

Table 1. Clinical and demographic characteristics of all participants.

	FXS group	ASD group	TD group	p value
Number of Participants	37 (34/3)	70 (47/23)	43 (28/15)	
Age (M ± SD)	4.35 ± 1.75	3.73 ± 1.34	4.25 ± 1.83	0.098 ^a
ADOS-2				
ADOS total score	15.42 ± 6.79	17.83 ± 4.34	NA	0.035
SA	12.03 ± 5.10	14.80 ± 3.75	NA	0.003
RRB	3.33 ± 2.07	2.03 ± 1.63	NA	0.428
CSS-total	5.70 ± 2.52	6.98 ± 1.58	NA	0.003
CSS-SA	5.79 ± 2.23	7.02 ± 1.79	NA	0.004
CSS-RRB	6.45 ± 1.90	5.95 ± 1.69	NA	0.186
GDS-C				
GDS average DQ	53.15 ± 18.45	60.88 ± 13.66	NA	0.013
Gross Motor DQ	61.63 ± 15.41	73.76 ± 14.32	NA	0.0001
Social DQ	49.82 ± 20.61	55.76 ± 15.22	NA	0.088
Language DQ	41.47 ± 26.07	45.15 ± 18.04	NA	0.384
Fine Motor DQ	55.76 ± 21.86	63.86 ± 15.20	NA	0.023
Performance DQ	58.73 ± 20.06	66.03 ± 17.86	NA	0.056

Data are mean (SD). All *p* values were obtained via independent *t* test (two-tailed), except the ANOVA test for age.

^aone-way ANOVA.

(DMN) during resting-state or specific tasks [9–11]. In contrast, fMRI research on FXS remains limited, largely due to its lower prevalence. One of the few task-based fMRI studies in FXS, which employed a facial-emotion discrimination task in individuals with FXS, revealed hypoactivation in the fusiform gyrus and hyperactivation in the medial and superior frontal cortex compared to ASD and typical developing controls [12, 13]. However, task-based fMRI presents challenges in these populations, as motor or cognitive differences may interfere with task performance (e.g., button-pressing demands), potentially obscuring core neural signatures. Resting-state fMRI (rs-fMRI) offers a valuable alternative by capturing intrinsic functional connectivity patterns, which reflect stable neurobiological traits rather than transient task-related states. This approach minimizes confounds related to task performance variability and allows for the identification of consistent connectivity alterations linked to baseline neuropathology. Recent resting-state fMRI studies have identified aberrant functional networks in children with FXS, such as the DMN, frontoparietal network (FPN), and dorsal attention network (DAN) [14, 15].

Findings from previous MRI studies have contributed to our understanding of the distinct neuroanatomical characteristics of ASD and FXS, yet the evidence for specific functional alterations and their relationship to behavior in these two disorders is very limited. Contrasting the functional alterations of key intrinsic brain networks, along with their relationship to relevant cognitive and behavioral phenotypes, will elucidate our understanding of the pathogenesis of both conditions and may provide important clues to rational approaches to targeted early intervention.

To bridge this gap, the present study aimed to examine the brain-behavior specificity by contrasting the resting-state functional network and behavior pattern of idiopathic ASD (a behaviorally defined developmental disorder) and FXS (a genetically defined disorder overlapping with cognitive and behavioral features of ASD), with typically developing controls. Our primary hypothesis is that children with FXS and ASD will display shared as well as distinct functional connectivity patterns. Considering that the cause of FXS is inherently different and more specific from that of idiopathic ASD, we further hypothesized that these two disorders may present substantially different brain-behavior associations.

METHODS

Participants

A total of 150 participants were consecutively recruited between January 2021 to August 2024 from Children's Hospital of Fudan University, China. Thirty-seven children (4.35 ± 1.75 years, 34/3) diagnosed with FXS confirmed by genetic testing (i.e., revealing more than 200 CGG repeats in the *FMR1* gene) were recruited (Supplementary material, Table S1). Seventy children (3.73 ± 1.34 years, 47/23) with ASD confirmed without a known genetic etiology were recruited as an idiopathic ASD group. ASD was diagnosed based on the Diagnostic and Statistical Manual of Mental Disorders, Fifth Edition (DSM-5) [16], and the Autism Diagnostic Observation Schedule, Second Edition (ADOS-2) [17] (Table 1). Forty-three typically developing (TD) children (4.25 ± 1.83 years, 28/15) exhibiting normal development were recruited as controls. Children with cerebral palsy, or other neurologic or degenerative diseases, or with recognizable lesions or abnormalities on scans confirmed by MRI, were excluded.

Assessments

Clinical assessments included physical and neurological examinations, evaluations of comorbidities, diagnostic evaluations (e.g. ADOS-2), and developmental and cognitive evaluations (e.g. GDS-C). For ADOS-2, Social Affect score (SA), Repeated and Repetitive Behavior score (RRB), as well as overall the Calibrated Severity Score (CSS) of SA and RRB were calculated to enable comparison of ADOS-2 scores across various modules. For GDS-C, overall developmental quotient (DQ) as well as DQ of subdomains including gross motor, fine motor, social, language and adaptability were calculated. The *FMR1* CGG repeats and methylation levels were tested (see details in Supplementary Materials - Methods).

MRI scans

All MRI scans were obtained on a GE 3.0 Tesla Discovery MR750 system (GE Medical Systems, Milwaukee, WI) with an 8-channel brain array coil. Parents were advised to skip their child's nap and keep them active the day before the scan to promote tiredness. On the scan night, children and parents rested in a dimly lit private room adjacent to the MRI facility, with scans initiated 15–20 min after sleep onset to ensure deep sleep. For some children in the FXS, ASD, or typically developing (TD) groups (e.g., those with incidental findings like delayed fontanelle closure or paroxysmal dizziness) who could not achieve natural sleep after two attempts, a low dose of chloral hydrate (50 mg/kg) was administered with parental consent and under the supervision of licensed clinicians or anesthesiologists. If a participant wakes up during the scan, one additional scan would be performed 10 min later (no further administration of chloral hydrate was

required). T1-weighted structural images of the brain were acquired sagittally using a 3D fast spoiled gradient echo (FSPGR) echo sequence (repetition time (TR) = 8.2 ms, echo time (TE) = 3.2 ms, flip angle = 12°, voxel size = $1 \times 1 \times 1 \text{ mm}^3$, FOV = 256 mm, matrix = 256×256 , scan duration = 510 s). Resting-state functional images were acquired using an echo planar imaging (EPI) sequence (TR = 2000 ms, TE = 30 ms, flip angle = 90°, FOV = 22.4 cm, resolution = 64×64 matrix, thickness = 3 mm, slices = 39, spacing = 0 mm, bandwidth = 250 kHz, scan duration = 400 s).

Image preprocessing

Preprocessing of images and regions of interest (ROIs)-based resting-state functional connectivity (rsFC) analysis was performed using the Data Processing & Analysis for Brain Imaging (DPABI) [18] and customized script (see details in Supplementary Materials - Methods).

We defined eight intrinsic function networks based on a well-defined functional parcellation derived from a sample of 1000 healthy participants [19]. These networks included the sensorimotor network (SMN), ventral attention network (VAN), visual network (VN), dorsal attention network (DAN), default mode network (DMN), and frontoparietal network (FPN). Since subcortical regions and cerebellum were often affected in FXS and ASD [20], we defined subcortical ROIs as the “subcortical network” (SCN) and cerebellum ROIs as the “cerebellum network” (CN). Information of the ROIs in each network was summarized in the supplementary material (Table S2).

Graph theory-based network topology analysis

To quantify the topological properties of rsFC networks, we calculated three key graph theory metrics for each node (ROI), including nodal degree, clustering coefficient, and nodal efficiency using Brain Connectivity Toolbox (<https://sites.google.com/site/bctnet/Home>). All metrics were computed within the whole-brain network consisting of all 160 ROIs. Nodal degree represents the total strength of functional connections linked to a node, reflecting its role as a potential hub for integrating information across the brain. Clustering coefficient captures the extent to which a node's neighboring regions are interconnected, indicating the local specialization of information processing within functional modules. Nodal efficiency measures the reciprocal of the shortest path lengths from a node to all other nodes, characterizing its capacity to support rapid communication with distant regions for global network integration [21]. Following previous approaches [14], these metrics were computed across a range of network densities (6–45%) to avoid biases from arbitrary threshold selection. The lower density bound ensured network connectivity without fragmentation, while the upper bound excluded non-specific connections. For each metric, we calculated the area under the curve (AUC) by integrating values over the entire density range. The AUC provides a threshold-independent summary of network topology, enhancing the robustness of group comparisons by accounting for dynamic changes in network organization across different sparsity levels.

Statistical analysis

All statistical analyses were controlled for age, head motion, and gender. The comparisons of network-level rsFC among all three groups employed general linear regression, with the mean FC of networks as the dependent variable and the group as the independent variable. Owing to the massive number of between- and with-network comparisons and their system-wide implications, we prioritized stringent statistical control for network-level analysis. Following previous neuroimaging studies [22, 23], post-hoc between-group comparisons of network-level were performed using independent t-tests at $p < 0.01$ to enhance the robustness and reproducibility of the distinct global FC patterns in FXS and ASD. For topological metrics exhibiting non-normal distributions, Kruskal-Wallis tests with Dunn's test were used to assess differences in global/local efficiency and nodal characteristics ($p < 0.05$). Multiple comparisons were addressed with false discovery rate correction using the Benjamini-Hochberg procedure.

To examine the potentially atypical patterns of brain-behavior associations in children with FXS and ASD, we calculated Spearman's correlation coefficient between different brain network measures and the multi-domain cognitive-behavioral measures. The differences in the patterns of brain-behavior associations in children with FXS and ASD were also tested through a z-test at a significant level of $p < 0.05$.

For the FXS group, we examined how the alterations in brain network properties were linked to individual methylation levels, a process that silences part of the *FMR1* gene and thus prevents it from generating its protein product (i.e., FMRP). Due to significant differences in methylation

levels between males and females, particularly the phenomenon of X-chromosome inactivation in females, which leads to considerable heterogeneity in the methylation status of the *FMR1* gene, we included only male children in this analysis.

RESULTS

Demographic characteristics of participants

The demographic information of the participants was summarized in Table 1. The age of the three groups did not exhibit a significant difference as examined by one-way ANOVA ($F = 2.363$, $p = 0.098$). For clinical symptoms, significant differences were found among the ASD and FXS groups on in several items of ADOS, including Calibrated Severity Score (CSS) (ASD vs. FXS, $t = 3.11$, $p = 0.003$), Social Affect score (SA) ($t = 3.066$, $p = 0.003$), CSS of SA ($t = 2.953$, $p = 0.004$) and GDC developmental domains of average DQ ($t = 2.499$, $p = 0.013$), gross motor DQ ($t = 4.05$, $p < 0.001$) and fine motor DQ ($t = 2.288$, $p = 0.023$).

Comparisons of within and between-network functional connectivity

Comparisons of mean FC calculated within and between the intrinsic brain networks showed significant group differences within the CN, DMN and 3 between-network FC, including DMN-CN, SMN-CN, VN-CN (Fig. 1B–D).

Decreased DMN FC in children with FXS. The DMN included 33 ROIs, as shown in Fig. 1A. Children with FXS demonstrated significantly decreased FC within the DMN network relative to the ASD and TD group ($F_{(2,147)} = 6.96$, $p = 0.009$; FXS vs. ASD: $p = 0.001$; FXS vs. TD: $p = 0.003$; ASD vs. TD: $p = 0.837$) (Fig. 1D). The groups did not differ significantly for within-network FC of other intrinsic networks (Supplementary material, Figure S1).

Decreased DMN-CN FC in children with ASD. For between-network FC comparisons among all three groups, children with ASD exhibited significantly decreased functional connectivity between DMN and CN compared to the TD group ($F_{(2,147)} = 10.337$, $p < 0.001$; FXS vs. ASD: $p = 0.138$; FXS vs. TD: $p = 0.023$; ASD vs. TD: $p < 0.0001$) (Fig. 1D).

Decreased CN, SMN-CN, VN-CN FC in children with FXS and children with ASD. The SMN included 29 ROIs whose connections with 33 ROIs in DMN are averaged and compared between groups (i.e. $29 \times 33 = 957$ connections). Both FXS and ASD groups showed significantly decreased functional connectivity in CN relative to the TD group ($F_{(2,147)} = 8.614$, $p = 0.003$; FXS vs. ASD: $p = 0.55$; FXS vs. TD: $p < 0.001$; ASD vs. TD: $p < 0.001$) (Fig. 1D). In addition, children with FXS and ASD exhibited significantly decreased FC between SMN and CN compared to the TD group ($F_{(2,147)} = 12.739$, $p < 0.001$; FXS vs. ASD: $p = 0.05$; FXS vs. TD: $p < 0.0001$; ASD vs. TD: $p < 0.001$) (Fig. 1D). We also found significantly decreased functional connectivity between the VN and CN in children with FXS and ASD compared to the TD group ($F_{(2,147)} = 15.123$, $p < 0.0001$; FXS vs. ASD: $p = 0.053$; FXS vs. TD: $p < 0.0001$; ASD vs. TD: $p < 0.0001$) (Fig. 1D).

Differences in brain network topology

Topological differences in children with ASD. Children with ASD showed alterations in network properties when evaluating the whole brain network composed of all 160 nodes. In terms of network efficiency, the AUC of global efficiency (E_{glob} , ASD vs. TD: $z = -2.618$, $p = 0.004$) and local efficiency (E_{loc} , ASD vs. TD: $z = -2.549$, $p = 0.005$) were significantly reduced in children with ASD in comparison to the TD group (Fig. 2A, B).

We also observed aberrant topological characteristics at different brain regions in the ASD and FXS groups, including crus I of the cerebellum, lobule IV-V of the cerebellum, right cuneus,

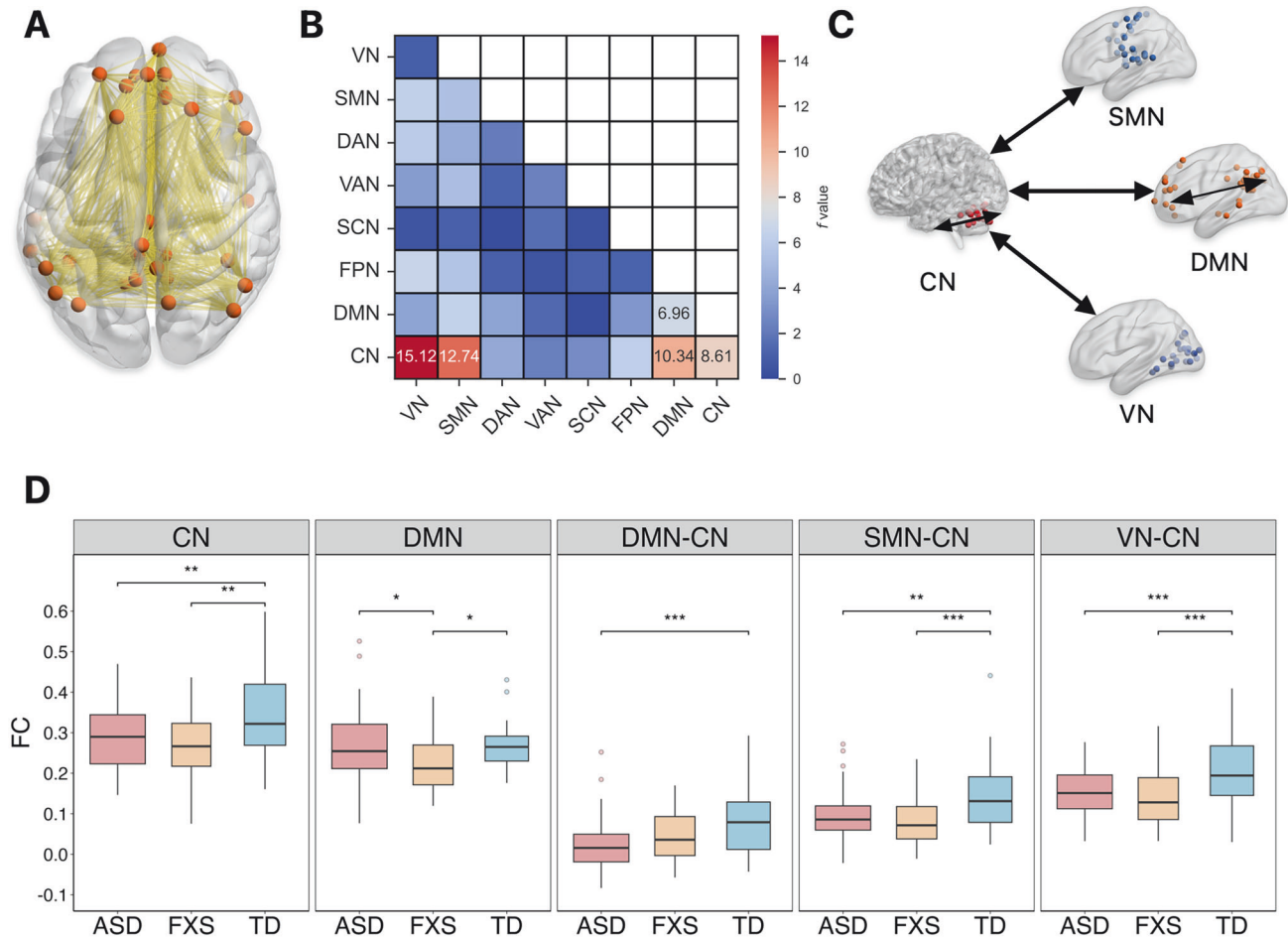


Fig. 1 Comparisons of mean FC within and between the intrinsic brain networks showed significant group differences. **A** Demonstration of the default mode network (33 ROIs); **B** All 36 large-scale network FC comparisons between ASD, FXS and TD groups. Squares with annotation of F value represent significantly altered large-scale network FC between the 3 groups (FDR corrected); **C** Significantly altered within- and between-network for the eight networks between ASD, FXS and TD groups; **D** Significant group differences in the mean FC of CN, DMN and between-network FC of DMN-CN, SMN-CN, VN-CN. VN visual network, SMN sensorimotor network, DMN default mode network, CN Cerebellum network. FDR-corrected p -value: *, $p < 0.01$; **, $p < 0.001$; ***, $p < 0.0001$. All statistical analyses were corrected for multiple comparisons using FDR (two-tailed).

left opercular cortex, and left precentral gyrus. Children with ASD displayed significantly decreased activity in these regions compared to the FXS and TD groups. In two cerebellar nodes, specifically, crus I exhibited a decreased degree, and lobule IV-V exhibited a decreased clustering coefficient in children with ASD compared to the TD group. (Crus I: ASD vs. TD: $p = 0.0002$; Lobule IV-V: ASD vs. TD: $p = 0.0012$). Similarly, children with FXS demonstrated lower nodal degree at the left Crus I of the cerebellum across different network densities compared with the TD groups (FXS vs. TD: $p < 0.0001$).

The AUC of the clustering coefficient of 3 nodes, including right cuneus, left opercular cortex and left precentral gyrus, was significantly lower in the ASD group compared to the FXS and TD groups (Cuneus: FXS vs. ASD: $p < 0.0001$, ASD vs. TD: $p = 0.0003$; Opercular cortex: FXS vs. ASD: $p = 0.002$, ASD vs. TD: $p < 0.0001$; Precentral gyrus: FXS vs. ASD: $p = 0.0017$, ASD vs. TD: $p < 0.0001$). In the FXS group, the AUC of the clustering coefficient at the left lobule IV-V of cerebellum was also significantly lower than the TD group (FXS vs. TD: $p = 0.0001$) (Fig. 2C, D).

Associations between intrinsic brain networks and developmental-behavioral measures

We conducted correlational analyses between ADOS-2 scores (specifically CSS-SA and CSS-RRB) and the aberrant FC we have

identified. Correlations between the mean FC of DMN-CN and both ADOS-2 scores (i.e., CSS-SA and CSS-RRB) in children with FXS significantly differed from those in the ASD group (CSS-SA: $z = 1.898$, $p = 0.029$; CSS-RRB: $z = 1.901$, $p = 0.029$, Fig. 3A).

A significant positive correlation was observed between the mean FC of SMN-CN and CSS-RRB in the FXS group ($r = 0.377$, $p = 0.037$). The correlations between the mean FC of SMN-CN and CSS-SA also significantly differed in ASD and FXS groups ($z = 1.687$, $p = 0.046$, Fig. 3B).

The correlation between the mean FC of VN-CN and CSS-SA also significantly differed in ASD and FXS groups ($z = 1.968$, $p = 0.025$, Fig. 3C).

Methylation level is associated with intrinsic networks in FXS

We classified boys with FXS into two groups based on their CGG repeat numbers in the *FMR1* gene. The first group (Full Mutation, FM) consisted of 21 boys with CGG repeat numbers exceeding 200, while the second group included 11 boys with CGG repeats both in the range of 55–200 and exceeding 200 (Mosaic, Pre/Full Mutation, PM/FM). Based on this grouping, we assessed the methylation levels of *FMR1* mRNA and found that the FM-only group showed significantly higher methylation levels than the PM/FM group ($p = 0.001$, Fig. 4A). The methylation levels demonstrated a significant negative correlation with the AUC of crus I's

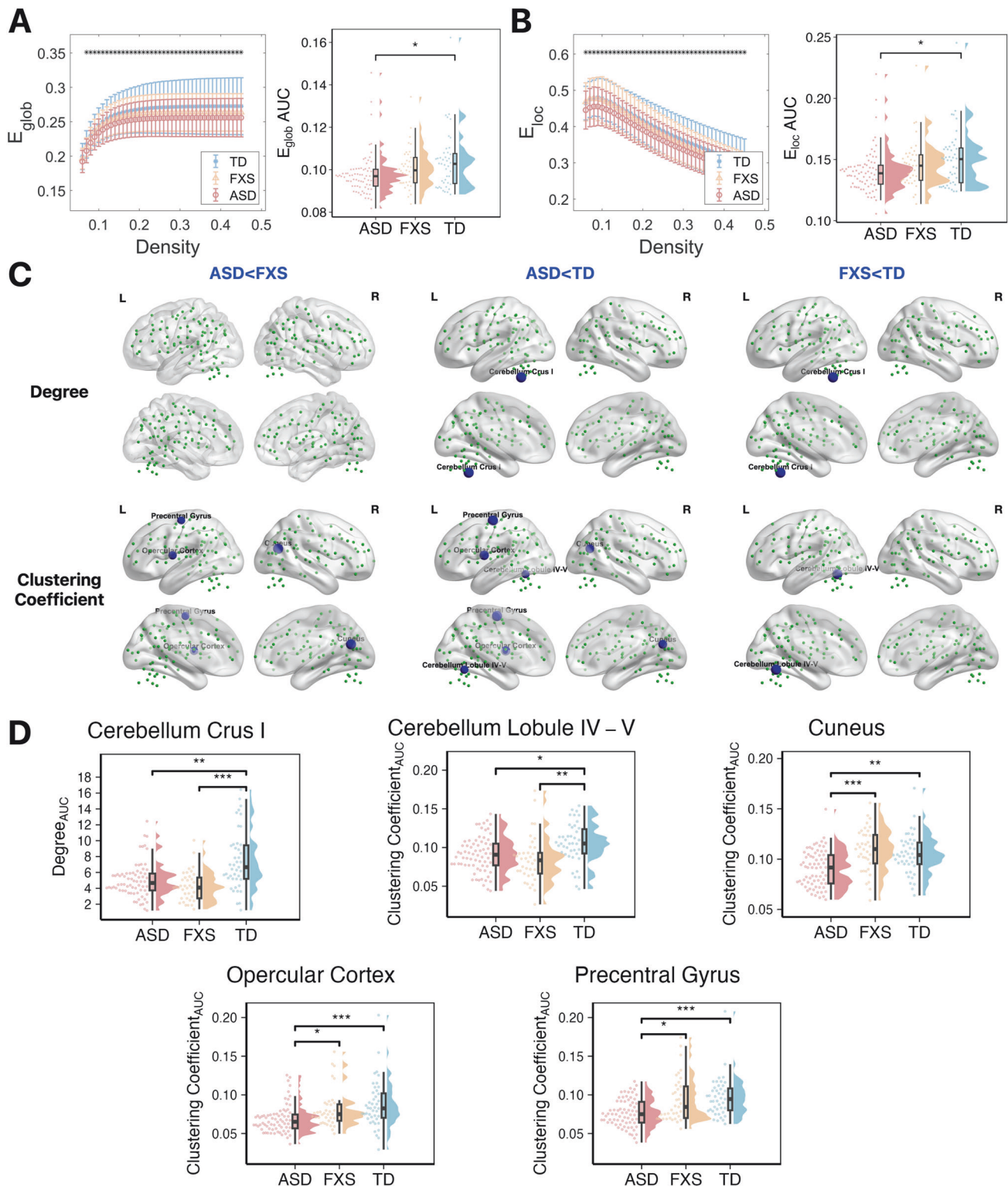


Fig. 2 Group differences in the network topological properties. **A** E_{glob} and its AUC across a density range between 6 and 45%. Each point and error bar denotes the mean and standard deviation at each density level, respectively. Asterisks indicate a significant difference in this density threshold. **B** E_{loc} and its AUC across a density range between 6 and 45%. **C** Group differences in AUC across a density range between 6 and 45% of degree, nodal efficiency, and clustering coefficient at the nodal level. Insignificant nodes are shown as green spheres, whereas blue (ASD < FXS, ASD < TD, FXS < TD) spheres denote significant differences after FDR correction at nodal level. **D** Post-hoc comparisons of nodes with significant differences of topological properties between groups. Post-hoc comparisons are conducted via Dunn's test. FDR corrected p -value: *, $p < 0.01$; **, $p < 0.001$; ***, $p < 0.0001$.

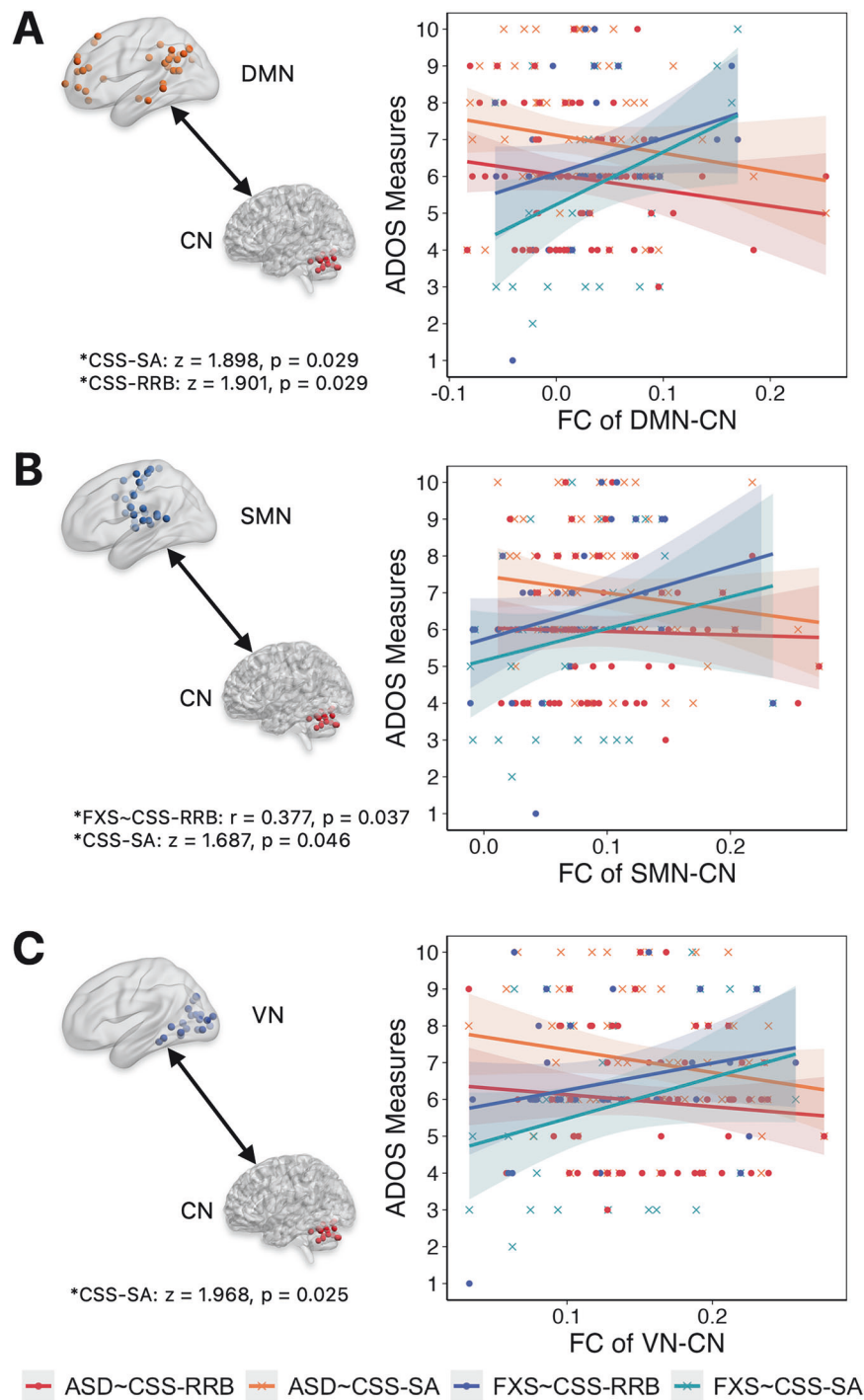


Fig. 3 Brain network functional connectivity and topological measures were correlated with multi-domain cognitive-behavioral characteristics assessed by ADOS-2. **A** Correlations between the mean FC of DMN-CN and CSS-SA, CSS-RRB in ASD and FXS groups. **B** Correlations between the mean FC of SMN-CN and CSS-SA, CSS-RRB in ASD and FXS groups. **C** Correlations between the mean FC of VN-CN and CSS-SA, CSS-RRB in ASD and FXS groups.

degree in the cerebellum (Fig. 4B). Several subgroup variances that approached significance are noteworthy. As shown in Fig. 4C, the FM group exhibited a trend towards decreased average DQ and language DQ as assessed by GDS-C.

DISCUSSION

The present study, for the first time, demonstrates both distinct and shared patterns of resting-state functional connectivity and

brain-behavior associations in young children with FXS and ASD, neurodevelopmental disorders that share overlapping behavioral phenotypes. Children with FXS demonstrated significantly suppressed within-network FC in the DMN compared to the ASD and TD controls. We also identified significantly suppressed within-network FC in the cerebellum network of the FXS and ASD groups relative to the TD group. These findings suggest the essential role of DMN in characterizing the neural profile of FXS and shared network alteration in both FXS and ASD. Aberrant between-

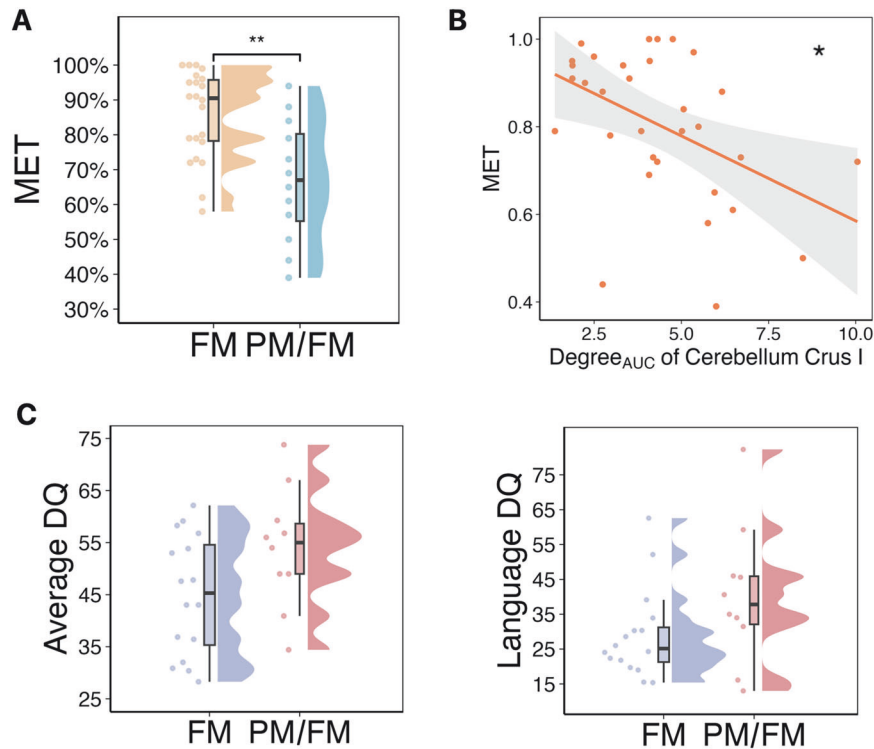


Fig. 4 Differences of subgroups in FXS defined by CGG type and their association with intrinsic brain networks. **A** Comparison of MET level between the subgroups of FXS ($t = -3.55$, $p = 0.001$). **B** Correlation between DegreeAUC of crus I and MET ($r = -0.434$, $p = 0.016$). **C** Comparison of average DQ ($t = -1.993$, $p = 0.058$) and language DQ ($t = -1.724$, $p = 0.098$) between subgroups of FXS. PM/FM pre/full mutation, FM full mutation.

network FC patterns among DMN, SMN, CN, and VN were found to significantly differentiate children with FXS and ASD from TD controls. In addition, key brain regions, including part of the cerebellum, VN (i.e., cuneus) and SMN (i.e., precentral gyri), showed different activity in children with ASD and FXS, indicating the distinctly aberrant topological properties in these two brain disorders. These findings add to the growing evidence that FXS and ASD, though sharing common phenotype profiles, are mainly characterized by distinctly different functional network patterns.

Children with FXS displayed significantly suppressed resting-state FC of DMN. Alterations of FC in DMN have been observed in FXS and ASD in previous studies [14, 24]. However, it remains unclear whether the altered FC patterns of the DMN are similar in both disorders. Our findings directly show that the FC of DMN is more severely impacted in FXS. It is well accepted that the DMN is active during the resting state by presenting strong activity, especially when individuals are focused on mental exploration of social and emotional content such as rumination, self-referential processing, and emotional appraisal [25, 26]. We can speculate that the cognitive and behavioral dysfunction in children with FXS may be distinctly related to the hypoactivity of the DMN in terms of recurrent and uncontrollable focus on socio-emotional processing in affected individuals.

We found that children with ASD and FXS share a common pattern of altered FC, as evidenced by their significantly decreased within-network and between-network FC compared to the TD group in several key networks. Both FXS and ASD groups reveal significant reductions in FC within the cerebellum network (CN). The cerebellum, traditionally recognized for its role in motor control, has increasingly been implicated in a variety of cognitive and affective processes [27, 28]. The observed decrease in FC within the CN in children with FXS and ASD suggests potential disruptions in these integrative functions. This aligns with previous studies indicating cerebellar abnormalities in both FXS and ASD

[29–31], which may contribute to the motor and cognitive deficits commonly observed in these populations. For instance, impairments in motor coordination, balance, and fine motor skills are frequently reported in children with FXS and ASD, and these may be linked to altered cerebellar connectivity [30–32]. In addition, the between-network FC, including SMN-CN, and VN-CN, were also significantly suppressed in FXS and ASD groups.

There is existing evidence of decreased FC involving visual, sensorimotor, and cerebellum networks in children with ASD [33, 34]. Consistent with this, we found significantly decreased FC between CN-SMN and between CN-VN in children with FXS and ASD. The SMN is crucial for processing sensory information and executing motor functions [35]. Reduced FC between the SMN and CN in children with FXS and ASD may reflect impairments in the coordination of sensory and motor activities. This could manifest as the motor coordination difficulties often reported in these children, further emphasizing the cerebellum's role in sensorimotor integration. On the other hand, the cerebellum's role in visual processing involves coordinating eye movements and integrating visual information with motor actions [27, 28, 30, 32]. Disruptions in VN-CN connectivity could lead to difficulties in tasks that require visual-motor coordination, such as catching a ball or navigating through space. Taken together, our findings may indicate the challenges in the coordination of motor functions and visuomotor adaptation in children with FXS and ASD [36, 37], shedding light on the underlying neural mechanism of motor difficulties and visual deficits often observed in these neurodevelopmental disorders.

The substantial network-level neural alterations in FXS and ASD may be attributed to specific regional alterations, as evidenced by the observed topological abnormality in these networks. In particular, children with FXS and ASD consistently demonstrated lower nodal degree in Crus I and lobule IV-V of the cerebellum compared to TD groups, a region crucial for motor coordination,

balance, and fine motor skills [28]. This regional alteration further supports the suppressed FC of CN observed in FXS and ASD groups, suggesting distinctive disruptions in the topology and connectivity of the cerebellum in these two disorders. Recent studies have linked cerebellar dysfunction to ASD and FXS, in which cerebellar region Crus1 was specifically linked to ASD and ASD-related behaviors in FXS [31, 38]. Our finding here aligns well with prior work, highlighting a critical role of the cerebellum as a shared biological basis for behavioral dysfunction in FXS and ASD. For the segregation property of brain network, children with ASD consistently exhibited suppressed regional segregation in the opercular cortex, precentral gyrus, and cuneus compared to other groups. These regions mainly integrate sensory and visual information, and motor coordination function [39–41]. We speculate that such distinct segregation disruptions in ASD may account for visual deficits and motor coordination challenges in ASD and underscores why children with ASD display different patterns of visual and motor dysfunction compared to those without ASD [32, 42].

Accumulated evidence has shown that RRB and SA severity often develop in parallel in individuals with ASD [35, 43]. However, individuals with FXS often exhibit a so-called “isolated SA-RRB” pattern where RRB changes relatively slowly regardless of SA severity [44, 45]. Interestingly, our data revealed a similar “isolated SA-RRB” pattern when correlating the SA and RRB severities with the FC between the CN and other representative intrinsic networks including DMN, SMN, and VN for the FXS group. Interestingly, the “isolated SA-RRB” pattern in FXS even revealed a significantly opposite trend compared with the ASD group. Previous studies have illustrated how the specific patterns of the between-network FC, such as CN-DMN, affect the cognitive dysfunctions in neuropsychiatric disorders [46–48]. These inter-network couplings are crucial for integrating motor coordination, self-referential processing, sensory and visual processing, suggesting a potential link between disrupted FC patterns and the manifestation of SA and RRB in FXS. Understanding the neural basis of this pattern may offer valuable insights into the pathophysiology of FXS and inform targeted interventions to address the specific cognitive and behavioral challenges faced by individuals with FXS.

Mosaicism in size and methylation is a prevalent phenomenon in FXS and has been observed to be associated with improved cognitive function [49]. However, this correlation is not universal, underscoring the intricate nature of the molecular and clinical profile in FXS. Surprisingly, the degree of the Crus-I region is negatively correlated with the methylation levels in children with FXS, implying that higher methylation is associated with more impaired regional connectivity in the cerebellum. This finding may offer evidence for linking cerebellar dysfunction and methylation with cognitive impairment in FXS since recent research has highlighted the cerebellum’s involvement in various cognitive and emotional processes [28, 31]. Together, our study represents the first to identify such a genetic-specific neural pattern within the FXS population. These findings shed light on the variability of the FXS phenotype, particularly in mosaic individuals, offering insights into the underlying mechanisms driving cognitive and behavioral outcomes in FXS.

Several limitations should be acknowledged in our study. First, due to the lower prevalence and unbalanced gender ratio of FXS, the overall sample size and female participants for the FXS group in our study are relatively small. Our finding may not generalize to females with FXS. Larger sample sizes and more female participants will be important to solidify the findings in the present study. We also expect that new methods will be proposed in the future to address the reliability challenges in investigations with relatively small sample sizes in disorders like FXS. In addition, the present study only investigated the cross-sectional characteristics of behavior and brain functional profiles of FXS and ASD.

These findings highlight the distinct and shared network alterations in children with FXS and ASD, which may hold implications for understanding their longitudinal developmental trajectories. For instance, reduced FC of the cerebellar network and aberrant topological properties (e.g., decreased nodal degree in Crus I and lobule IV-V) were observed in both groups. These cerebellar disruptions, particularly in regions critical for sensorimotor integration and cognitive-affective processing, could serve as early biomarkers for predicting longitudinal motor and cognitive outcomes and advancing the development of individualized treatment. In future investigations, longitudinal designs tracking cerebellar FC alongside behavioral outcomes are critical to validate these hypotheses.

DATA AVAILABILITY

Access to the identified participant research data must be approved by the research ethics board on a case-by-case basis, please contact the corresponding authors (xujiong@fudan.edu.cn, rihuili@um.edu.mo, zqiao@fudan.edu.cn) for assistance in data access request.

REFERENCES

- Bhat S, Acharya UR, Adeli H, Bairy GM, Adeli A. Autism: cause factors, early diagnosis and therapies. *Rev Neurosci*. 2014;25:841–50.
- Volkmar FR, McPartland JC. From kanner to DSM-5: autism as an evolving diagnostic concept. *Annu Rev Clin Psychol*. 2014;10:193–212.
- Manoli DS, State MW. Autism spectrum disorder genetics and the search for pathological mechanisms. *Am J Psychiatry*. 2021;178:30–8.
- Hagerman R, Hoem G, Hagerman P. Fragile X and autism: intertwined at the molecular level leading to targeted treatments. *Mol Autism*. 2010;1:12.
- Mei L, Hu C, Li D, Wang Y, Li H, Zhang K, et al. The incidence and clinical characteristics of fragile X syndrome in China. *Front Pediatr*. 2023;11:1064104.
- Schumann CM, Carter Barnes C, Lord C, Courchesne E. Amygdala enlargement in toddlers with autism related to severity of social and communication impairments. *Biol Psychiatry*. 2009;66:942–9.
- Shen MD, Swanson MR, Wolff JJ, Elison JT, Girault JB, Kim SH, et al. Subcortical brain development in autism and fragile X syndrome: evidence for dynamic, age- and disorder-specific trajectories in infancy. *Am J Psychiatry*. 2022;179:562–72.
- Hazlett HC, Poe MD, Lightbody AA, Styner M, MacFall JR, Reiss AL, et al. Trajectories of early brain volume development in fragile X and autism RH: trajectory of brain volume in fragile X. *J Am Acad Child Adolesc Psychiatry*. 2012;51:921–33.
- Cooper RA, Richter FR, Bays PM, Plaisted-Grant KC, Baron-Cohen S, Simons JS. Reduced hippocampal functional connectivity during episodic memory retrieval in autism. *Cereb Cortex*. 2017;27:888–902.
- Kennedy DP, Courchesne E. The intrinsic functional organization of the brain is altered in autism. *Neuroimage*. 2008;39:1877–85.
- Iidaka T, Kogata T, Mano Y, Komeda H. Thalamocortical hyperconnectivity and amygdala-cortical hypoconnectivity in male patients with autism spectrum disorder. *Front Psychiatry*. 2019;10:252.
- Bruno JL, Garrett AS, Quintin EM, Mazaika PK, Reiss AL. Aberrant face and gaze habituation in fragile X syndrome. *Am J Psychiatry*. 2014;171:1099–106.
- Dalton KM, Holsen L, Abbeduto L, Davidson RJ. Brain function and gaze-fixation during facial emotion processing in fragile-X and autism. *Autism Res*. 2008;1:231–9.
- Li R, Lightbody AA, Lee CH, Bartholomay KL, Marzelli MJ, Reiss AL. Association of intrinsic functional brain network and longitudinal development of cognitive-behavioral symptoms in young girls with fragile X syndrome. *Biol Psychiatry*. 2023;94:814–22.
- Saggar M, Bruno JL, Hall SS. Brief intensive social gaze training reorganizes functional brain connectivity in boys with fragile X syndrome. *Cereb Cortex*. 2023;33:5218–27.
- Diagnostic and statistical manual of mental disorders: DSM-5™. 5th ed. Arlington, VA, US: American Psychiatric Publishing, Inc.; 2013. xlv, 947 p. (Diagnostic and statistical manual of mental disorders: DSM-5™, 5th ed).
- Lord C, Rutter M, Goode S, Heemsbergen J, Jordan H, Mawhood L, et al. Autism diagnostic observation schedule. *J Autism Dev Disord*. 2012;284:474–8.
- Yan CG, Wang XD, Zuo XN, Zang YF. DPABI: data processing & analysis for (resting-state) brain imaging. *Neuroinformatics*. 2016;14:339–51.
- Thomas Yeo BT, Krienen FM, Sepulcre J, Sabuncu MR, Lashkari D, Hollinshead M, et al. The organization of the human cerebral cortex estimated by intrinsic functional connectivity. *J Neurophysiol*. 2011;106:1125–65.
- Lightbody AA, Reiss AL. Gene, brain, and behavior relationships in fragile X syndrome: evidence from neuroimaging studies. *Dev Disabil Res Rev*. 2009;15:343–52.

21. Rubinov M, Sporns O. Complex network measures of brain connectivity: uses and interpretations. *Neuroimage*. 2010;52:1059–69.
22. Yu A, Gao Q, Deng Z, Dang Y, Yan C, Chen Z, et al. Common and unique alterations of functional connectivity in major depressive disorder and bipolar disorder. *Bipolar Disord*. 2023;25:289–300.
23. Yang H, Chen X, Chen ZB, Li L, Li XY, Castellanos FX, et al. Disrupted intrinsic functional brain topology in patients with major depressive disorder. *Mol Psychiatry*. 2021;26:7363–71.
24. Uddin LQ, Supekar KS, Ryali S, Menon V. Dynamic reconfiguration of structural and functional connectivity across core neurocognitive brain networks with development. *J Neurosci*. 2011;31:18578–89.
25. Broyd SJ, Demanuele C, Debener S, Helps SK, James CJ, Sonuga-Barke EJS. Default-mode brain dysfunction in mental disorders: a systematic review. *Neurosci Biobehav Rev*. 2009;33:279–96.
26. Buckner RL, Andrews-Hanna JR, Schacter DL. The Brain's default network. *Ann N Y Acad Sci*. 2008;1124:1–38.
27. Koziol LF, Budding D, Andreassen N, D'Arrigo S, Bulgheroni S, Imamizu H, et al. Consensus paper: the Cerebellum's role in movement and cognition. *Cerebellum*. 2014;13:151–77.
28. Rudolph S, Badura A, Lutz S, Pathak SS, Thieme A, Verpeut JL, et al. Cognitive-affective functions of the cerebellum. *J Neurosci*. 2023;43:7554–64.
29. Huber KM. The fragile X–cerebellum connection. *Trends Neurosci*. 2006;29:183–5.
30. Chen Y, Guo L, Han M, Zhang S, Chen Y, Zou J, et al. Cerebellum neuropathology and motor skill deficits in fragile X syndrome. *Int J Dev Neurosci*. 2022;82:557–68.
31. Gibson JM, Vazquez AH, Yamashiro K, Jakkamsetti V, Ren C, Lei K, et al. Cerebellar contribution to autism-relevant behaviors in fragile X syndrome models. *Cell Rep*. 2023;42:113533.
32. Lim YH, Licari M, Spittle AJ, Watkins RE, Zwicker JG, Downs J, et al. Early motor function of children with autism spectrum disorder: a systematic review. *Pediatrics*. 2021;147:e2020011270.
33. Xu S, Li M, Yang C, Fang X, Ye M, Wei L, et al. Altered functional connectivity in children with low-function autism spectrum disorders. *Front Neurosci*. 2019;13:806.
34. Lepping RJ, McKinney WS, Magnon GC, Keedy SK, Wang Z, Coombes SA, et al. Visuomotor brain network activation and functional connectivity among individuals with autism spectrum disorder. *Hum Brain Mapp*. 2022;43:844–59.
35. Wang P, Kong R, Kong X, Liégeois R, Orban C, Deco G, et al. Inversion of a large-scale circuit model reveals a cortical hierarchy in the dynamic resting human brain. *Sci Adv*. 2019;5:eaa7854.
36. Oldehinkel M, Mennes M, Marquand A, Charman T, Tillmann J, Ecker C, et al. Altered connectivity between cerebellum, visual, and sensory-motor networks in autism spectrum disorder: results from the EU-AIMS longitudinal european autism project. *Biol Psychiatry Cogn Neurosci Neuroimaging*. 2019;4:260–70.
37. Tzvi E, Loens S, Donchin O. Mini-review: the role of the cerebellum in visuomotor adaptation. *Cerebellum*. 2022;21:306–13.
38. Kelly E, Meng F, Fujita H, Morgado F, Kazemi Y, Rice LC, et al. Regulation of autism-relevant behaviors by cerebellar–prefrontal cortical circuits. *Nat Neurosci*. 2020;23:1102–10.
39. Măliia MD, Donos C, Barborica A, Popa I, Ciurea J, Cinatti S, et al. Functional mapping and effective connectivity of the human operculum. *Cortex*. 2018;109:303–21.
40. Banker L, Tadi P. Neuroanatomy, precentral gyrus. StatPearls [Internet]. Treasure Island (FL): StatPearls Publishing; 2024. <http://www.ncbi.nlm.nih.gov/books/NBK544218/> [cited 2024 Sep 20].
41. Palejwala AH, Dadario NB, Young IM, O'Connor K, Briggs RG, Conner AK, et al. Anatomy and white matter connections of the lingual gyrus and cuneus. *World Neurosurg*. 2021;151:e426–37.
42. Nebel MB, Eloyan A, Nettles CA, Sweeney KL, Ament K, Ward RE, et al. Intrinsic visual-motor synchrony correlates with social deficits in autism. *Biol Psychiatry*. 2016;79:633–41.
43. Lawson LP, Joshi R, Barbaro J, Dissanayake C. Gender differences during toddlerhood in autism spectrum disorder: a prospective community-based longitudinal follow-up study. *J Autism Dev Disord*. 2018;48:2619–28.
44. Hagerman RJ, Harris SW. Autism profiles of males with fragile X syndrome. *Am J Ment Retard*. 2008;113:427–38.
45. Thurman AJ, McDuffie A, Kover ST, Hagerman RJ, Abbeduto L. Autism symptomatology in boys with fragile X syndrome: a cross sectional developmental trajectories comparison with nonsyndromic autism spectrum disorder. *J Autism Dev Disord*. 2015;45:2816–32.
46. Guo W, Liu F, Xiao C, Zhang Z, Yu M, Liu J, et al. Dissociation of anatomical and functional alterations of the default-mode network in first-episode, drug-naïve schizophrenia. *Clin Neurophysiol*. 2015;126:2276–81.
47. Wang Z, Wang Y, Sweeney JA, Gong Q, Lui S, Mosconi MW. Resting-state brain network dysfunctions associated with visuomotor impairments in autism spectrum disorder. *Front Integr Neurosci*. 2019;13:17.
48. Unruh KE, Bartolotti JV, McKinney WS, Schmitt LM, Sweeney JA, Mosconi MW. Functional connectivity of cortical-cerebellar networks in relation to sensorimotor

behavior and clinical features in autism spectrum disorder. *Cereb Cortex*. 2023;33:8990–9002.

49. Jiraanont P, Kumar M, Tang HT, Espinosa G, Hagerman PJ, Hagerman RJ, et al. Size and methylation mosaicism in males with fragile X syndrome. *Expert Rev Mol Diagn*. 2017;17:1023–32.

ACKNOWLEDGEMENTS

This work was supported by grants from the National Natural Science Foundation of China (82171540, 82301743), the Science and Technology Development Fund of the Macao SAR (0010/2023/ITP1), the University of Macau (SRG2023-00015-ICI), Natural Science Foundation of Anhui Province (No.2308085MH255), grant funds of China Medical Board (CMB) (22–471), foreign expert program of Ministry of Science and Technology (G2022132004L), academic leaders development program of Children's Hospital of Fudan University (EKXDPY202306). We thank J. Wang and B. Yang, for MRI sequence adaptation and image scanning. We also thank P. Dong and W. Lu for transferring patients to us. We also thank L. Mei and Y. Zhu for contacting patients and their families. This work was performed in part at SICC which is supported by SKL-IOTSC, University of Macau. The content is solely the responsibility of the authors and does not necessarily represent the official views of the Children's Hospital of Fudan University or the University of Macau.

AUTHOR CONTRIBUTIONS

QX, RL and ZQ designed the study. CH, YT, XX, DL contributed to the acquisition of research data. DL and DF conducted the data analysis. QX, RL, ZQ and DL provided the interpretation of results. DL and DF wrote the first draft of the manuscript. AR and RH revised the manuscript.

COMPETING INTERESTS

The authors declare no competing interests.

ETHICS APPROVAL AND CONSENT TO PARTICIPATE

The study was conducted in compliance with the declaration of Helsinki, approved by the Ethics Committee of Children's Hospital of Fudan University (approval number: 2021-312). Written informed consent was obtained from all participants (or their legal guardians) after detailed information notification before participation in the study.

ADDITIONAL INFORMATION

Supplementary information The online version contains supplementary material available at <https://doi.org/10.1038/s41380-025-03112-y>.

Correspondence and requests for materials should be addressed to Zhongwei Qiao, Rihui Li or Qiong Xu.

Reprints and permission information is available at <http://www.nature.com/reprints>

Publisher's note Springer Nature remains neutral with regard to jurisdictional claims in published maps and institutional affiliations.



Open Access This article is licensed under a Creative Commons Attribution-NonCommercial-NoDerivatives 4.0 International License, which permits any non-commercial use, sharing, distribution and reproduction in any medium or format, as long as you give appropriate credit to the original author(s) and the source, provide a link to the Creative Commons licence, and indicate if you modified the licensed material. You do not have permission under this licence to share adapted material derived from this article or parts of it. The images or other third party material in this article are included in the article's Creative Commons licence, unless indicated otherwise in a credit line to the material. If material is not included in the article's Creative Commons licence and your intended use is not permitted by statutory regulation or exceeds the permitted use, you will need to obtain permission directly from the copyright holder. To view a copy of this licence, visit <http://creativecommons.org/licenses/by-nc-nd/4.0/>.